Journal of Applied Pharmaceutical Science Vol. 14(06), pp 218-230, June, 2024
Available online at http://www.japsonline.com
DOI: 10.7324/JAPS.2024.168894
ISSN 2231-3354

In vitro studies on curcumin-loaded multiwalled carbon nanotubes antioxidant activities and cytotoxicity against Hep G-2 liver cancer cell lines

Manar Rabba'a[1], Rund Abu-Zurayk[2,3*], Bashaer Abu-Irmaileh[3], Saida Abu Mallouh[3], Yasser Bustanji[4,5,6*]

[1]Biology Department, School of Science, The University of Jordan, Amman, Jordan.
[2]Nanotechnology Center, The University of Jordan, Amman, Jordan.
[3]Hamdi Mango Center for Scientific Research, The University of Jordan, Amman, Jordan.
[4]Research Institute of Medical and Health Sciences, University of Sharjah, Sharjah, United Arab Emirates.
[5]College of Medicine, University of Sharjah, Sharjah, UAE.
[6]School of Pharmacy, The University of Jordan, Amman, Jordan.

ARTICLE HISTORY

Received on: 10/01/2024
Accepted on: 26/04/2024
Available Online: 05/06/2024

Key words:
Curcumin, chitosan, carbon nanotubes, drug delivery system, nanotechnology, MWCNT.

ABSTRACT

Many nanoscale drug delivery systems have been evaluated for their excellent properties, such as carbon nanotubes; however, due to their hydrophobic nature, surface modification or functionalization is the major step to prepare a biocompatible and well-dispersed multiwalled carbon nanotubes (MWCNTs) in biological fluids. This study aims to noncovalently functionalize MWCNT with chitosan to deliver curcumin to liver cancer cell lines and to investigate their *in vitro* cell cytotoxicity and antioxidant activity. The conjugation between chitosan, MWCNT, and curcumin was confirmed using Fourier transform infrared spectroscopy, Brunauer–Emmett–Teller surface area, pore size analysis, scanning electron microscopy, and thermogravimetric analysis. It was found that curcumin-chitosan-MWCNT had the highest entrapment efficiency of 99.1%. The average surface area of curcumin-chitosan-MWCNT was 52.73 m^2/g, which showed more than 80% antioxidant activity for all used concentrations using 2,2-Diphenyl-1-picrylhydrazyl and 2,2′ azinobis, 3-ethylbenzothiazoline-6-sulphonic acid methods. The IC 50 of curcumin-chitosan-MWCNT used on the Hep G2 liver cell line was 43.62 µg/ml, while it was 227.6 µg/ml when used on fibroblast. In conclusion, the combination of curcumin, chitosan, and MWCNT showed a considerable reduction in cancer cell viability, and curcumin-chitosan-MWCNT can be proposed as a biocompatible carrier for liver cancer treatment.

INTRODUCTION

The perfect drug delivery system involves selective controlled release and effective targeted delivery of the proposed drug to minimize systemic toxicity [1]. The use of nanocarriers, such as carbon nanotubes (CNTs), gold, silver, dendrimers, polymeric nanoparticles, liposomes, and polymeric nanoparticles, as innovative and adaptable platforms in drug delivery systems, has received a lot of interest [1–7]. These nanoscale architectures provide numerous advantages, such as enhanced drug stability, controlled release, targeted administration into cancer cells, increased bioavailability, and the potential for combination therapy. Due to their nanoscale width, innovative hollow structure, and exceptional physicochemical properties, CNTs have received a lot of attention as potential drug carrier systems [1]. CNTs can easily penetrate living cells without causing any damage or demise. However, because of their weak dispersibility in aqueous solutions, their pharmacological applications were restricted. CNTs may be functionalized to overcome their low dispersibility, enhance their selective dispersion, and increase their controlled release and cell penetration [1,8]. Multiwalled carbon nanotubes (MWCNTs), are a common type of CNTs

*Corresponding Author
Rund Abu-Zurayk, Nanotechnology Center, The University of Jordan, Amman, Jordan.
E-mail: r.abuzurayk @ ju.edu.jo
Yasser Bustanji, Research Institute of Medical and Health Sciences, University of Sharjah, Sharjah, United Arab Emirates.
E-mail: ybustanji @ sharjah.ac.ae

that can be used in different pharmaceutical applications. Liquid oxidation of MWCNT produces functional groups (hydroxyl and carboxyl) on the surface of MWCNT [1,9]. These functional groups could be used as extra sites for further functionalization or addition reaction [9,10]. Liquid phase oxidation allows the introduction of oxygenated functional groups on MWCNTs' surface, which is performed using hydrogen peroxide (H_2O_2), hydrogen peroxide: sulfuric acid combination (H_2O_2:H_2SO_4), nitric acid (HNO_3), or nitric acid: sulfuric acid mixture (HNO_3: H_2SO_4) [11].

They enhance the decrement of long-range van der Waals attraction forces and the increment of MWCNT-matrix/solvent interaction which results in homogenous dispersion [12]. Therefore, MWCNT functionalization causes reactivity enhancement, and solubility improvement, and provides a path for further MWCNT chemical modifications such as metal deposition, ion adsorption, and grafting reactions. Furthermore, the functional groups work as anchor groups for two moieties connection and are more deriving by chemical reactions with other functional groups [13–15]. Functionalization of MWCNT renders them more compatible with organic solvents to prevent aggregation and permit better dispersion and solubilization within the polymer matrix. MWCNTs can be also modified through noncovalent interaction between polymers and CNTs to form polymer/CNT nanocomposites. Chitosan is one of the widespread polymers that is used in CNT modification and in medical applications due to its suitable bioactivity and biological properties [3,5,16–18]. Curcumin is a natural lipophilic polyphenol derived from rhizomes of the *Curcuma longa*, a perennial plant that belongs to the ginger family Zingiberaceae. Its molecular formula is $C_{21}H_{20}O_6$, with 368.38 Da. Curcumin has many pharmacological and therapeutic activities, including antitumor, antiproliferative, antioxidant, antimicrobial, anti-inflammatory, anti-obesity, anti-metastasis, dietary agent, pro-apoptotic, neuroprotective, and hepatoprotective activities [19–25]. The poor bioavailability of curcumin is a crucial challenge in its applications due to its chemical instability, low water solubility, poor absorption, and rapid metabolism [26]. Due to its hydrophobic properties, most of the orally consumed curcumin does not get absorbed into the small intestine epithelium cells [27]. Furthermore, due to the rapid metabolism of curcumin after oral administration, most of it is degraded in tissues such as the liver and small intestine before entering systemic circulation [26].

In this study, MWCNT was synthesized to improve the water-solubility of hydrophobic curcumin. Depending on the simple conjugation between curcumin's hydroxyl group and MWCNT's carboxyl group via a hydrogen bond, curcumin will be activated to inhibit cell growth. To the best of our knowledge, there are no previous studies about linking curcumin with MWCNTs to test the improved curcumin's antioxidant activity and cytotoxicity against the liver HepG-2 cancer cell line.

MATERIALS AND METHODS

Materials

MWCNTwith (95% purity, 30–50 nm outside diameter, and 10–20 μm length) were purchased from US Research Nanomaterials, Inc. USA. Nitric acid (70 wt.%) was obtained from (CARLO ERBA, France). Sulfuric acid (98 wt.%), Anhydrous N, N-Dimethylformamide (DMF) 99.8%, oxalyl chloride ≥99%, and curcumin powder (cat # of C1386, Lot. # SHBL0796) were purchased from (Sigma Aldrich, Beijing, China). Low molecular weight chitosan (Genochem World, Batch # 412QEG). Dulbecco's phosphate-buffered saline (PBS) (pH 7.4, Euro clone, Cat no. ECB4004L). Dimethyl sulfoxide (DMSO) cell culture reagent was obtained from (Santa Cruz Biotechnology, USA). Cellulose membrane filters (0.45 μm pore diameter), glacial acetic acid, NaOH, nitrogen gas, absolute ethanol, KBr, acetate buffered solution (pH 5.5) prepared according to US Pharmacopeia, 2,2-Diphenyl-1-picrylhydrazyl (DPPH), ascorbic acid, 2,2′ azinobis, 3-ethylbenzothiazoline-6-sulphonic acid ($ABTS^+$), potassium persulfate ($K_2S_2O_8$), and the dye solution [3- (4,5-dimethylthiazol-2-yl) 2,5-diphenyltetrazolium bromide] (MTT) was obtained from (Promega, USA). MTT kit, fibroblast cell line, HepG-2 (liver cancer cell line), Iscove's media, EMEM media (EuroClone S.p.A Italy), Gibco™ Roswell Park Memorial Institute (RPMI) 1640 Medium, fetal bovine serum (PAN ™ Biotech, South America), penicillin–streptomycin solution 100× (EuroClone S.p.A Italy), trypsin (Biowest the serum specialist), and MEM nonessential amino acids 100× (EuroClone S.p.A Italy).

Methods

Oxidation of MWCNTs

To oxidize MWCNTs, a mixture of sulfuric acid and nitric acid in a volume ratio of 1:3 was used. 0.2 g of MWCNTs were dispersed in this acid mixture and then refluxed for 24 hours at 70°C and 350 rpm. The resulting suspension was diluted with distilled water to a volume of 1,000 ml, filtered through a 0.45 μm cellulose membrane, and repeatedly washed to remove any remaining acid. The acid-free MWCNTs were then exfoliated from the membrane and dried in an oven at 70°C for 72 hours. [28,29].

Functionalization of MWCNT by chitosan

The chitosan-MWCNT composite was prepared using two methods: a solution processing method by mixing a dispersion of oxidized MWCNT with chitosan solution according to Sobh *et al*. [1], and by chemical functionalization by oxalyl chloride under nitrogen gas according to Bozeya *et al*. [28]. The drug loading was achieved by combining the required amount of drug (curcumin) with ethanolic dispersions of both chitosan-MWCNT and oxidized-MWCNT at room temperature, each in dark conditions and in light conditions.

MWCNT functionalization by solution processing method

Low molecular weight chitosan (5 mg/ml) was dissolved in 1% (*v*/*v*) glacial acetic acid, mixed with 2.5 g/ml of oxidized MWCNTs, sonicated for 20 minutes, stirred for 48 hours. at room temperature, then 1% (*w*/*v*) NaOH was used to collect chitosan bounded with MWCNTs (Chitosan-MWCNT), washed several times with deionized water, centrifuged at 4,000 rpm and 4°C to remove any unbounded chitosan, and then allowed to dry at room temperature [1].

Chemical functionalization of MWCNT by oxalyl chloride

A mixture of 120 mg of previously prepared oxidized MWCNT and 80 ml of DMF was sonicated for 20 minutes, then

1 ml oxalyl chloride was added drop-wise to the suspension under nitrogen gas. This mixture was stirred at 350 rpm in an ice bath for 2 hours, then it was stirred at room temperature for another 2 hours, followed by overnight stirring at 70°C to remove excess oxalyl chloride.

After that, a mixture composed of 490 mg of low molecular weight chitosan and 40 ml of DMF was sonicated for 20 minutes, then added to the previous mixture (MWCNT, DMF, and oxalyl chloride) and stirred for 48 hours at 110°C. The resulting mixture was then filtrated and washed until no chitosan residues remained in the filtrate; finally, the particles were vacuum dried for 4 hours [28].

Loading of curcumin into MWCNTs

Forty milligrams of oxidized MWCNT, chitosan-MWCNT, and chitosan-MWCNT-oxalyl-Cl each were solely dispersed in 20 ml of absolute ethanol, sonicated for 30 minutes. This step was repeated for two different batches each, as it was applied under dark and light conditions. Forty milligrams of curcumin powder were weighed in 6 tubes, each one was dispersed in 20 ml of absolute ethanol, and sonicated for 30 minutes. Then, the two solutions (curcumin and MWCNT) were mixed, sonicated for 30 minutes, and stirred at 350 rpm for at least 16 hours on either dark or light to load the curcumin on the surface of MWCNTs (Table 1).

Each solution was centrifuged at 4°C and 3,000 rpm for 10 minutes and the supernatant was used to measure the loading efficiency with the aid of a spectrophotometer at 428 nm, whereas the resulting combinations were listed in Table 1. Samples were washed with deionized water and dried at room temperature for further use [1].

Determination of curcumin loading efficiency onto MWCNT

The supernatant resulting from the previous step was diluted to 1:1,000 and the absorbance of the diluted sample was measured at 428 nm, using a spectrophotometer. The loading efficiency was calculated according to Equation (1) [30].

$$\text{Loading efficiency} = \frac{\text{Ct-Cs}}{\text{Ct}} \times 100\% \quad (1)$$

where Ct is the total amount of curcumin used and Cs is the amount of curcumin in the supernatant.

Determination of curcumin entrapment efficiency onto MWCNT

To measure the entrapment efficiency of curcumin on MWCNTs, ethanolic dispersions with a concentration of 1 mg/ml were prepared for each treatment previously listed in Table 1, each dispersion was prepared, sonicated for 20 minutes, and then centrifuged in 4°C at 4,000 rpm for 30 minutes. The absorbance of curcumin in the supernatant (free drug) was measured by spectrophotometer at 428 nm according to Figure 1 which shows the curcumin spectrum. Then, the entrapment efficiency of curcumin in each drug was measured using Equation 2 [30].

$$\text{Entrapment efficiency} = \frac{\text{WCi-WCf}}{\text{WCi-WCf}} \times 100\% \quad (2)$$

where WC_i is the initial weight of curcumin and WC_f is the weight of free curcumin.

Characterization

Fourier transform-infrared spectroscopy (FTIR)

FTIR was performed to check for oxidation using a Thermo Nicolet NEXUS 670 (Gaithersburg, MD, USA), using 32 scans over the range 4,000–400 cm^{-1} with 4.0 cm^{-1} resolution. Samples were characterized using KBr [28].

Scanning electronic microscope

Sample morphology and the examination of nanotube alignment were investigated using Scanning electron microscope (SEM). The analysis was performed using SEM QUANTA FEG 450 instruments. Samples were placed on aluminum stubs, sputtered with gold (5 nm thickness), and analyzed with appropriate magnification using Inspect™ F50 apparatus.

Thermogravimetric analysis (TGA)

To confirm the attachment of biomolecules to the surface of CNTs A METTLER TOLEDO TGA/SDTA851ᵉ was used to determine the thermal stability of pristine MWCNT, oxidized-MWCNT, chitosan, curcumin, chitosan-MWCNT, curcumin-chitosan-MWCNT, and curcumin-MWCNTs by heating (2–3) mg of each sample from 25°C to 1,000°C at a rate of 10°C/minute in a nitrogen atmosphere [31].

Brunauer–emmett–teller (BET) surface area analysis

The surface area of samples was measured by Quantachrome Nova 2200e series device. Before analysis, samples of oxidized-MWCNT, curcumin-chitosan-MWCNT,

Table 1. Loading conditions of curcumin on either MWCNT alone or chitosan-MWCNT.

Drug combination		Loading condition
Curcumin	Oxidized-MWCNT	Light
		Dark
Curcumin	Chitosan-MWCNT (Solution processing)	Light
		Dark
Curcumin	Chitosan-MWCNT (oxalyl-Cl)	Light
		Dark

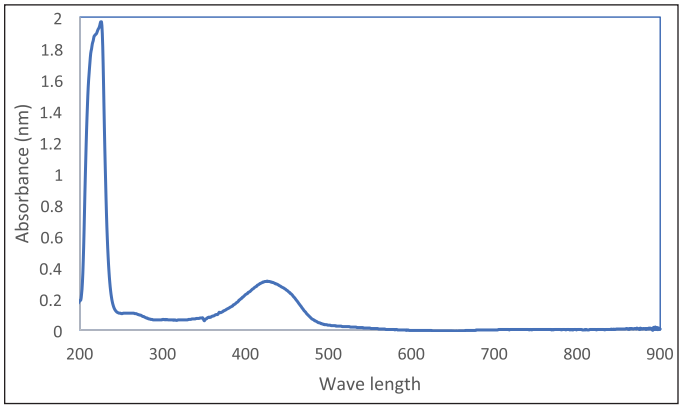

Figure 1. Curcumin spectrum using UV-Vis spectrophotometer.

and curcumin-MWCNTs were degassed at 105°C for 20 hours. Measurements of surface area and pore size distributions of the degassed samples were determined by using pure nitrogen gas as adsorbed in liquid nitrogen (77 K) [29].

Antioxidant activity

Determination of antioxidant activity using the DPPH radical scavenging assay. The antioxidant activity of the oxidized-MWCNT, chitosan, curcumin, chitosan-MWCNT, curcumin-chitosan-MWCNT, and curcumin-MWCNT against DPPH was determined using the previously described method [32–34]. A methanolic-DPPH solution with a concentration of 0.6 mM was mixed with 8 dilutions of each sample starting from 1,000 until 7.8 µg/ml as follows: 120 µl sample was added to 240 µl methanol along with 120 µl of 0.6 mM DPPH solution so the concentrations were divided by 4 to reach the final concentration loaded in the 96 well plates. Three replicates per sample and concentration were used. The mixture was kept in the dark for 30 minutes at room temperature and the absorbance was measured at 517 nm using an ELIZA plate reader. The methanolic dilution of DPPH was used as a negative control, while the Ascorbic acid was used as a positive control. DPPH radical scavenging activity of each sample and concentration was measured by Equation 3:

$$\text{DPPH scavenging \%} = \frac{\text{Absorbance of control-Absorbance of sample}}{\text{Absorbance of control}} \times 100\% \quad (3)$$

The reducing ability of an antioxidant compound was quantitatively determined by decolorizing the violet color of the DPPH solution which was recorded as absorbance change at 517 nm using an ELIZA plate reader. This feature presets to reduce the DPPH in solution by an antioxidant substance as it gives an electron or hydrogen, causing the DPPH lighter in color, measured in terms of its absorbance. The higher the antioxidant concentration the lesser the absorbance of reagent.

Determination of antioxidant activity using the $ABTS^+$ radical scavenging assay. The antioxidant assay of oxidized-MWCNT, chitosan, curcumin, chitosan-MWCNT, curcumin-chitosan-MWCNT, and curcumin-MWCNT was determined by using $ABTS^+$. Radical $ABTS^+$ was prepared through the oxidation of $ABTS^+$ by potassium persulfate ($K_2S_2O_8$).

A mixture (1:1 *v*/*v*) of $ABTS^+$ (7 mM) and potassium persulfate (2.45 mM) was prepared and kept in the dark for 16 hours at room temperature. 16 Serial dilutions were made for all previous 6 combinations starting from 10,000 ppm. 600 µl from various concentrations of oxidized-MWCNT, chitosan, curcumin, chitosan-MWCNT, curcumin-chitosan-MWCNT, and curcumin-MWCNT solutions was mixed with 60 µl $ABTS^+$ solution, and absorbance was measured at 734 nm against a blank (PBS) [35]

Each concentration was analyzed three times. The average radical scavenging assay of samples was calculated through Equation 4:

$$\text{RS\%} = \frac{\text{Abs control-Abs sample}}{\text{Abs control-Abs sample}} \times 100\% \quad (4)$$

where Abs control is the absorbance of control and Abs sample is the absorbance of the sample.

$ABTS^+$ is considered the best free radical reagent to be used to measure the electron/hydrogen donating potential of natural substances and is also an appropriate substrate for enzymes like peroxidases [36].

Anti-cancer activity

Cytotoxicity test. The effects of oxidized MWCNT, chitosan, curcumin, chitosan-MWCNT, curcumin-chitosan-MWCNT, and curcumin-MWCNT on the viability of fibroblast cells (control), and HepG-2 (liver cancer cell line), were evaluated using viability/cytotoxicity (MTT colorimetric assay) kit that analyzes the integrity of mitochondrial function by producing formazan crystals, which are proportionally related to the cell viability as the higher crystal production, exhibit higher cell viability [37,38]. Each cell line was cultured in 96-well plates in its appropriate media as follows: (fibroblast in Iscove's media, while HepG-1 in EMEM media) which were supplemented with 10% (*v*/*v*) fetal bovine serum and antibiotics (penicillin-streptomycin). The cells were cultured at 37°C in a humidified atmosphere of 5% CO_2/95% air. When the cells reached 80% confluency, they were trypsinized, counted, then calculated to be 8,000 cells /well, and plated in 96-well culture plates, where they were incubated overnight. Stock solutions (1 mg/ml) of oxidized-MWCNT, chitosan, curcumin, chitosan-MWCNT, curcumin-chitosan-MWCNT, and curcumin-MWCNTs were prepared by dissolving the formulations in DMSO. Afterward, it was diluted in the appropriate media to different concentrations (400, 200, 100, 50, 25, and 12.5 µg/ml), the cells were treated with a 100 µl aliquot of each concentration for the next 72 hours. At the end of this incubation period, the media in each well was replaced by 100 µl of RPMI and 10 µl of MTT solution. After 3 hours 100 µl of the solubilization stop solution was added to each well. Then, after at least 1 hour the absorbance was measured using an ELIZA microplate reader at 570 nm. Results were quantified as relative values to that of the negative control, where the negative control (untreated cells) was set to 100% viability. All experiments were performed in triplicate.

From the absorbance data, the IC50 (concentration that induces half the maximum effect) was calculated using graph pad prism software. The percentage of cytotoxicity was measured according to Equation 5:

$$\text{Cell viability \%} = \frac{\text{Absorbance of treated cells}}{\text{Absorbance of untreated cells}} \times 100\% \quad (5)$$

Statistical analysis

Quantitative data were expressed as the mean ± standard error of the mean. Differences between the groups were analyzed using an analysis of variance in GraphPad Prism statistical software, and $p < 0.05$ was considered statistically significant.

RESULTS AND DISCUSSION

Oxidation, functionalization, loading, and entrapment efficiency of curcumin on MWCNTs

MWCNT oxidation by acid refluxing is expected to remove the catalyst impurities and result in the production

of MWCNT-COOH [39,40]. The carboxylic acid group was successfully exposed to the MWCNT surface according to the FTIR spectrum (Fig. 2).

Polymeric MWCNT nanocomposites were produced by MWCNT encapsulation with the natural polymer chitosan (biodegradable and biocompatible) to be used as anticancer drug delivery systems. The aim of encapsulation is to achieve the most efficient delivery of bioactive molecules by monitoring sustained prolonged release at the target sites [1]. In addition, chitosan-based nanoparticles increase drug penetration through the narrow junction into the bloodstream toward the specific site [41]. The highest loading efficiency of curcumin on either oxidized-MWCNT or chitosan-MWCNT was estimated to be 54% for curcumin-MWCNT loaded at room temperature and light conditions, whereas 99.1% was the highest entrapment efficiency for chemically functionalized chitosan-MWCNT with the aid of oxalyl chloride under light conditions as mentioned in Table 2.

Low values of loading may result from the steric hindrance between curcumin and chitosan conjugated on oxidized MWCNTs surface which limits the loading of curcumin [42] also acid oxidation of CNT usually uses a high concentration of acids facilitated by heating (refluxing), and ultrasonication to produce CNT dispersion (mechanical forces). However, they frequently lead to disintegration because of severe cuts in the nanotubes. Shortening the CNTs may not allow sufficient load transfer of drug molecules [43].

The high entrapment efficiency in all treatments (Table 2) may be because, in the presence of absolute ethanol, curcumin was fully exposed to the MWCNT surface. In addition, the curcumin molecular structure, which contains two benzene rings and a conjugated ethylenic linkage, allowed curcumin to be easily adsorbed onto MWCNT or attached to it, under the ultrasonic bath energy, and the ultrasonic probe, through the formation of hydrogen bonds between the carboxyl groups of the functionalized MWCNTs and the phenolic hydroxyl group of curcumin. Along with hydrogen bonds, the van der Waals interactions between MWCNT and curcumin enhance curcumin entrapment as they are both hydrophobic [44].

Characterization results

Fourier transform-infrared spectroscopy

FT-IR spectra were used to assess the chemical structure and the exposed functional group on the surface of pristine MWCNT, the oxidized-MWCNT, chitosan, curcumin, chitosan-MWCNT prepared in both solution processing method and chemical functionalization using oxalyl-chloride, curcumin-chitosan-MWCNT, and curcumin-MWCNT using 32 scans over the range 4,000–400 cm^{-1} with 4.0 cm^{-1} resolution. Samples were characterized using KBr (Fig. 2). FT-IR spectra of pristine MWCNTs represented six distinct peaks for the functional groups on the pristine-MWCNT surface which were O–H, C–H, O=C=O, C=C, C-N stretching, and C-H bending. The absorption bands at 3,543, 3,466, and 3,417 cm^{-1} refer to O-H stretching. The presence of the hydroxyl group could be due to the surrounding atmospheric moisture or to manufacturing methods that can introduce the hydroxyl group

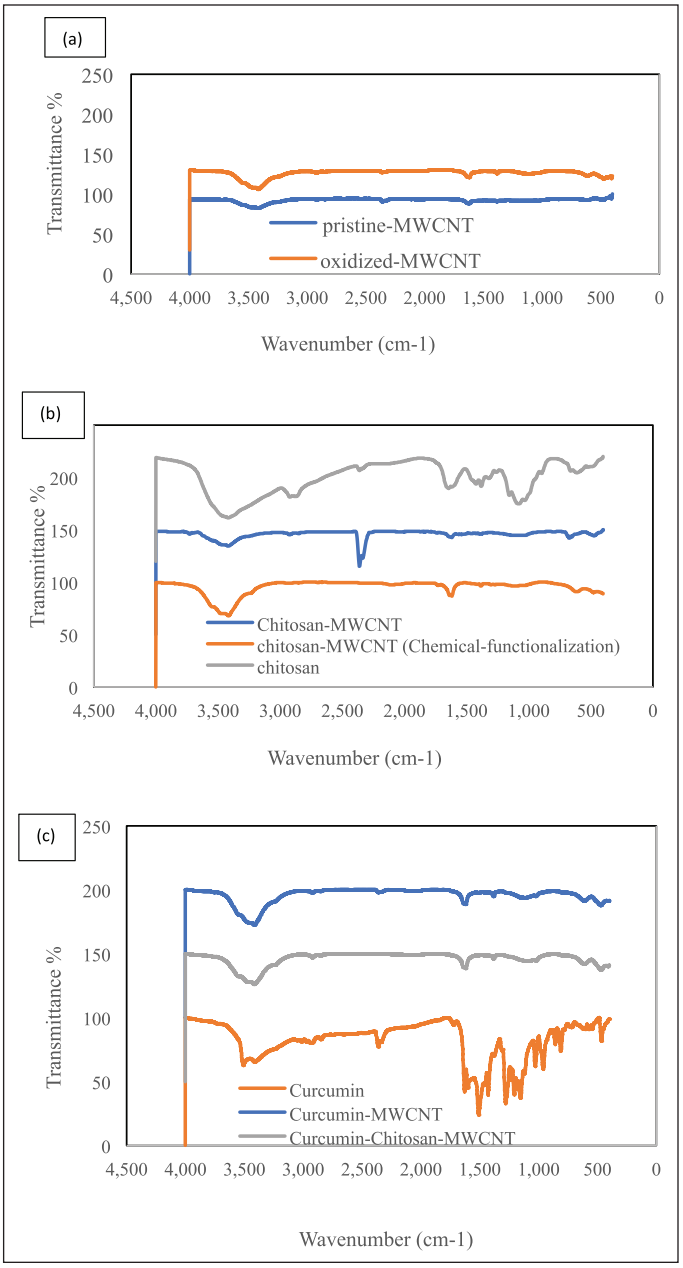

Figure 2. The FTIR spectra of (a) pristine-MWCNTs and oxidized-MWCNTs, (b) chitosan and chitosan-MWCNT, and (c) curcumin, curcumin-MWCNT, and curcumin-chitosan-MWCNT.

Table 2. Curcumin loading and entrapment efficiency results.

Drug combination		Loading condition	Loading efficiency %	Entrapment efficiency %
Curcumin	MWCNT	Light	54	80.9
		Dark	48.5	93.6
Curcumin	Chitosan-MWCNT (Solution processing)	Light	33.3	98
		Dark	27.3	96.7
Curcumin	Chitosan-MWCNT (oxalyl-Cl)	Light	34.7	99.1
		dark	38.7	97.4

through the purification process [11], while the absorption band at 2,918 cm^{-1} is associated with C-H stretching, which agreed with Abdolmaleki *et al*. [45] who get a peak on 2,922 cm^{-1} for MWCNT defects. All peaks located between 2,840–3,000 cm^{-1} are attributed to C-H stretching, whereas the absorption bands at 2,360, 1,618, and 1,381 cm^{-1} are associated with O=C=O stretching, C=C stretching, and C-H bending, respectively, as shown in Figure 2.

For the oxidized-MWCNT FT-IR spectra (Fig. 2), the peaks at 3,548, 3,473, 3,413, and 3,234 cm^{-1} correspond to O–H stretching, while the peaks at 2,918 and 2,852 cm^{-1} were related to C-H stretching. The stretch peak located at 2,362 and 2,852 cm^{-1} correspond to O=C=O stretching. As the gas phase product of MWCNTs was validated to be CO_2, the peak located at 1,722 corresponds to the presence of C=O stretching which is considered due to oxidation forming the COOH groups on the surface of MWCNTs. The peak at 1,618 cm^{-1} corresponds to C=C stretching which could be assigned as the stretching of the CNT backbone [45], the peak at 1,383 cm^{-1} is related to C-H bending, at 1,132 a new peak related to C-O stretching of a secondary alcohol, and a peak of C-N stretching located at 1,020 cm^{-1} is also observed. The FTIR spectra demonstrated that the pristine-MWCNTs had been oxidized to the point where they had alcohol and carboxylic acid groups on their surface before being functionalized with chitosan. The oxidation of reactive defects produced after exposing the pristine MWCNTs to a mixture of nitric acid and sulfuric acid may result in the formation of these functionalities [46].

The bands located between 3,570 and 3,200 cm^{-1} demonstrated the presence of a hydroxyl group, while the peaks between 2,935 and 2,840 cm^{-1} were attributed to methylene C-H stretching. The peaks between 2,360 and 2,335 cm^{-1} in FT-IR spectra of pristine-MWCNT, and oxidized MWCNT, were corresponding to O=C=O stretching, since CO_2 is considered as the gas phase product of MWCNT; therefore, CO_2 is the product of pristine and modified MWCNTs after oxidation while the presence of vibrational peaks at CO_2 location in the spectra of chitosan, solution-processed chitosan-MWCNT, curcumin, and curcumin-MWCNT appeared due to environmental factors since the samples should not contain CO_2 [47,48]. The emerged peak at 2,079 cm^{-1} in the FT-IR spectra of chemically functionalized chitosan-MWCNT attributed to the presence of N=C=S isothiocyanate. The peaks between 1,760 and 1,700 cm^{-1} were attributed to C=O, while the bands located between 1,650–1,600 cm^{-1} and 1,690–1,675 cm^{-1} represented the presence of conjugated alkene C=C stretching for the MWCNT backbone [45,48,49]. An aldehyde C-H bending was demonstrated for the peaks located between 1,390 and 1,380 cm^{-1}, while between 680 and 610 cm^{-1} an alkyne C-H bending appeared, in addition, a secondary amine C-N stretching peaks also existed at 1,090–1,020 cm^{-1} [45,48,50].

The IR Spectra data clearly indicated the presence of both curcumin and chitosan on the oxidized MWCNT. It is noted that the main characteristic peaks for functional groups in both MWCNT and the produced combination appeared in the Spectra after loading. This is in agreement with Sobh *et al*. [1], who noted the presence of main peaks characteristic for functional groups in both of free drug and the produced chitosan-MWCNT loaded with curcumin, when observing the presence of a peak at 3,220 cm^{-1} for O-H vibration of a carboxyl group and at 1,040 cm^{-1} is the stretching vibration of C-O. Whereas when combining chitosan with MWCNT, a stretching vibration of N-H appeared at 3,480 cm^{-1} while a C=O stretching was vibrated at 1,040 cm^{-1} in the CONH, which confirms that the chitosan was grafted onto MWCNT via amide linkage which comes in accordance with our results for oxidized MWCNT at a wavenumber of 3,230 and 1,020 cm^{-1} stretching peaks of –OH vibration of the carboxyl group and C-O stretching was appeared, respectively, while for curcumin-chitosan-MWCNT, a vibration peak for N–H stretching was noted at 3,477 and at 1,018 cm^{-1} a vibration of C=O stretching in the CONH appeared, which confirms the amide linkage between the curcumin and the chitosan-MWCNT.

Scanning electron microscopy

There are two clear aspects to be observed when examining the SEM image of pristine MWCNT (Fig. 3); the entanglement and the severe agglomeration of pristine MWCNTs forming cotton-like agglomerates [51–53]. The SEM image of pristine MWCNT shows hollow straight tubes with different size distributions and those tubes form a bundle of tangled tubes with smooth surfaces and compact sidewalls.

After oxidation of pristine MWCNT with a mixture of strong acids, the SEM micrograph (Fig. 3) shows clear intact single tubular threads-like MWCNT with a wider average diameter, rougher surface structure, less entangled MWCNTs, and agglomerates. It also maintains the whole structure with no collapse after the oxidation [53,54]. The roughness on the surface of oxidized MWCNT is due to the formation of defect sites because of oxygenated functional groups' attachment on their surface after acid treatment [55]. The severe structural damage also associated with the used-strong oxidizing acids which attack the existing active sites on the walls of CNTs may also be due to the mixture scission effect and high treating temperature during refluxing [55]. There were no obvious impurities traces appearing on oxidized MWCNT as the used pristine MWCNT was of 95% purity and acid treatment was responsible for the removal of any impurities traces [55,56]

SEM observation of oxidized-MWCNT functionalized with chitosan and loaded with curcumin showed less structural damage on its surface, as they were shortened, and their surface became more layered. The curvy MWCNTs in various size distributions with some aggregations shown in SEM micrographs that is probably due to the presence of intermolecular forces sticking the tubes together [52,53].

Thermal degradation analysis of functionalized CNTs

Generally, CNT thermal deterioration involves three stages, the first stage is moisture release, the second stage involves the structural deterioration of functional groups on the CNT surface, and the third one involves the oxidation of remaining carbon [57]. Figures 4 illustrates the TGA graphs of pristine-MWCNTs, oxidized-MWCNT, chitosan, chitosan-MWCNT, curcumin, curcumin-MWCNT, and curcumin-chitosan-MWCNT. At 703°C, Pristine-MWCNTs start to lose some of their weight due to the decomposition of the associated

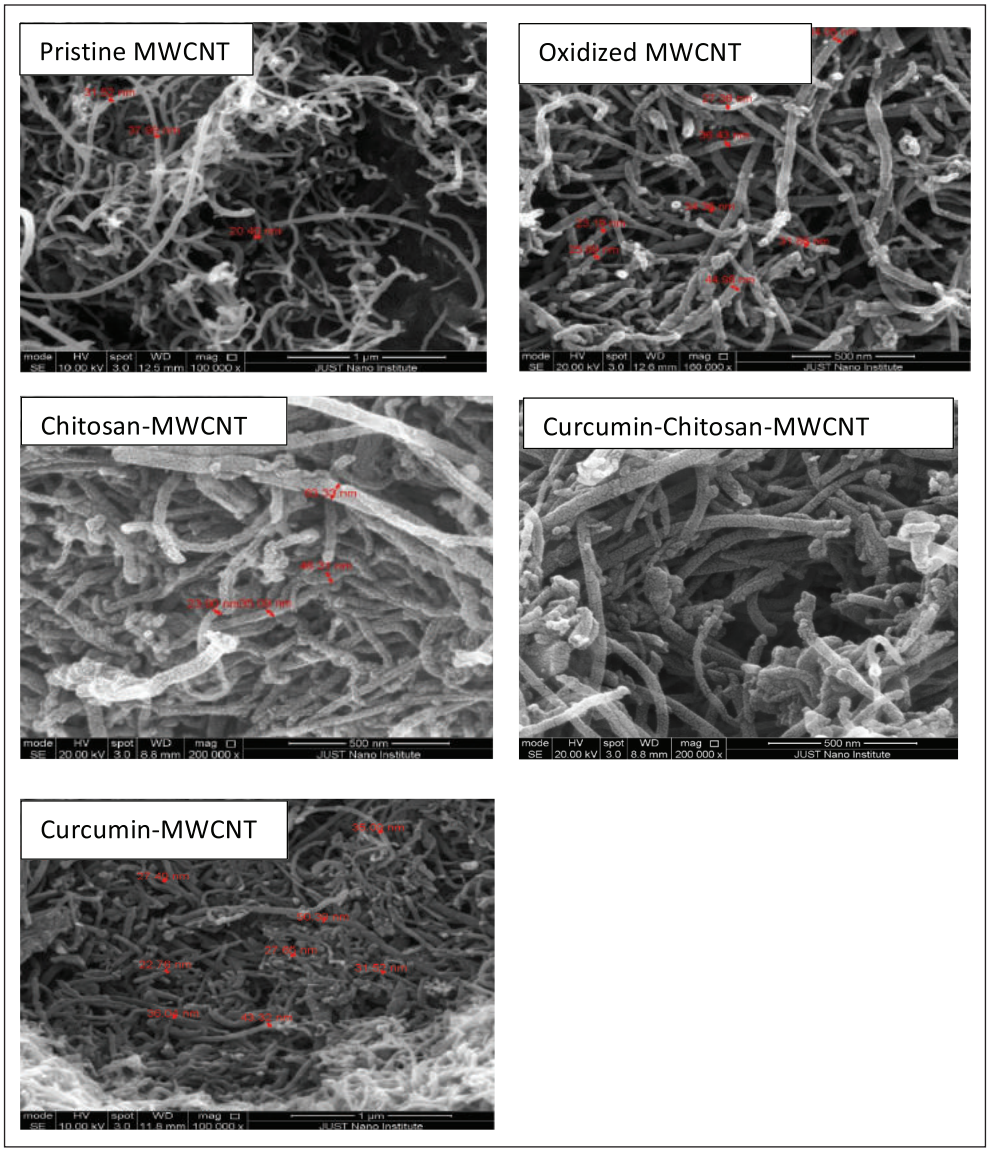

Figure 3. SEM of pristine-MWCNT (magnification scale bar 1 µm), oxidized MWCNT (500 nm scale bar), chitosan-MWCNT (500 nm scale bar), curcumin-chitosan-MWCNT(500 nm scale bar), and curcumin-MWCNT(500 nm scale bar).

organic groups [58], while the oxidized-MWCNTs start to lose some of their weight when reaching 800°C. There was a progressive weight loss above 700°C and 800°C for Pristine-MWCNTs and oxidized-MWCNTs, respectively. This loss could be attributed to the removal of oxygen-containing groups such as hydroxyl groups that arose during the CNT production and oxidation processes [9,11]. The low weight loss amount may be attributed to the purity of the sample used [59]. With increasing temperature, the gradual small amount of weight loss for both pristine-MWCNT and oxidized MWCNT is probably due to the small amount of moisture absorbed by the adsorbent [60]. Chitosan lost approximately 5% of its weight between 75°C and 260°C, due to water evaporation, while the major weight loss (approximately 50%) occurred between 260°C and 340°C, which was attributed to the breaking of the glycosidic linkages during chitosan degradation [61]. When comparing the thermal behavior of chitosan with chitosan-MWCNTs; between 300°C and 800°C, chitosan-MWCNT started to lose approximately 5% of its weight due to water evaporation while when reaching 996°C approximately 10% of its weight was lost due to depolymerization of chitosan and decomposition of the carboxylic group (−COOH) of MWCNT releasing oxygen into the TGA chamber [58,62]. This confirms the successful grafting of MWCNT into chitosan via the solution processing method as the presence of MWCNT resulted in the increase of thermal stability of chitosan-MWCNT [1,9]. This result comes in accordance with Sobh *et al*. [1] who reported that chitosan was the least thermal stable sample during studying the thermal stability of chitosan, and chitosan-MWCNT before loading the curcumin, or 5-fluorouracil, where the thermal stability increased with the addition of MWCNT [63].

Regarding Curcumin thermal stability, it has been shown to be stable up to 70°C for 10 minutes, while above 70°C, curcumin began degradation, and at 100°C its decomposition rate increased [64]. Loading of curcumin on MWCNT or on chitosan-MWCNT enhances the curcumin thermal stability, while binding of curcumin with MWCNT is slightly less thermally stable than its binding with chitosan-MWCNT which led to a slight increase in thermal stability, and this agreed with Sobh *et al*. [1] who studied the thermal stability of curcumin when bounded to chitosan functionalized MWCNT and they found that the combination between chitosan-MWCNT and curcumin is thermally stable.

BET: surface area and pore size analysis

The surface area, total pore volume, and average pore diameter of oxidized MWCNT, curcumin-MWCNT, and curcumin-chitosan-MWCNT are given in Table 3. As seen in Table 3, the increase in BET surface area of oxidized-MWCNT compared to curcumin-MWCNT and curcumin-chitosan-MWCNT may be due to the removal of impurities during the oxidation process and moisture blocking the pores during the carboxylation process [29,39]. From a different angle, the inclusion of curcumin and chitosan into MWCNT can be attributed to the decrease in surface area of curcumin-chitosan-MWCNT in contrast to oxidized-MWCNT. The MWCNT's accessible surface area is decreased as a result of this integration, which is consistent with research done in 2020 by Aghababaei *et al*. [65]. In comparison to pure MWCNT, the curcumin-chitosan-MWCNT, and curcumin-MWCNT composites are observed to have larger average pores. This finding shows that the MWCNT structure has been deformed as a result of the modification process. This discovery is in line with work done by Doğan *et al*. [39], who combined modified hexagonal-boron nitride nanoparticles with modified MWCNTs for hydrogen storage and found comparable outcomes.

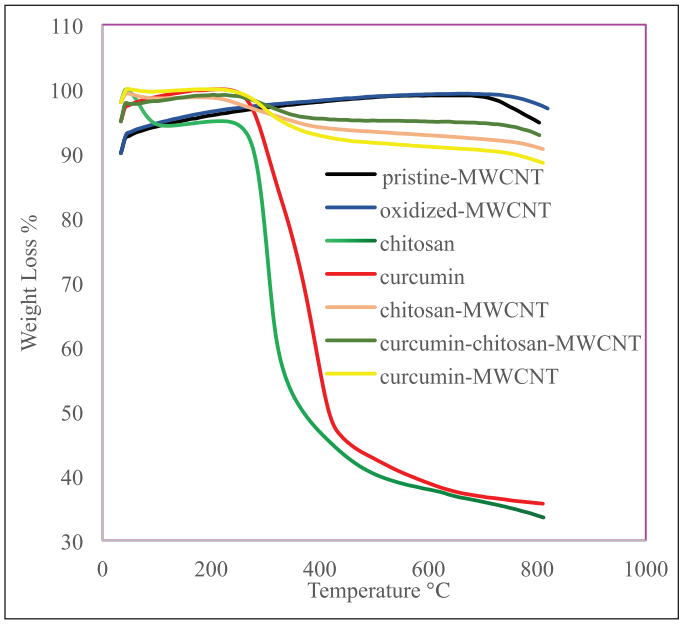

Figure 4. TGA thermographs of chitosan, chitosan-MWCNT, curcumin, curcumin-MWCNT, and curcumin-chitosan-MWCNT.

Table 3. BET surface areas, total pore volume, the average pore diameter of oxidized MWCNT, curcumin-MWCNT, and curcumin-chitosan-MWCNT.

Sample name	BET surface area (m^2/g)	Total pore volume (cc/g)	Average pore diameter (°A)
Oxidized-MWCNT	88.77	0.168	75.6
Curcumin-MWCNT	72.97	0.186	102.1
Curcumin-chitosan-MWCNT	52.73	0.145	109.9

Determination of antioxidant activity using both DPPH and $ABTS^+$ radical scavenging assays

In this study, the antioxidant activities of oxidized-MWCNT, chitosan, curcumin, chitosan-MWCNT, curcumin-MWCNT, curcumin-chitosan-MWCNT, and ascorbic acid which was used as positive control were examined using 1,1-diphenyl-2-picrylhydrazyl radical (DPPH) and 2,2′ -azino-bis-(3-ethylbenzothiazoline-6-sulfonic acid) diammonium salt ($ABTS^+$) methods. DPPH results are shown in Figure 5, and $ABTS^+$ results are shown in Figure 6. MWCNT exhibited strong antiradical properties [66]. Oxidation of MWCNT exposes the carboxyl group on the surface of MWCNT as it has been proposed that surface functionalization of MWCNT with carboxyl group will improve MWCNT free-radical scavenging activity [67]. An inverse relationship was obtained for MWCNT and their RS%; increasing MWCNT concentration decreased RS% as shown in Figures 5 and 6. The RS ability of chitosan and chitosan-MWCNT has a direct relationship with concentration. This result comes in line with Tomida *et al*. [68] who studied the antioxidant activity of seven different types of chitosan depending on their molecular weight and found that increasing the chitosan concentration increased their scavenging rate. Furthermore, chitosan's scavenging ability may be attributed to the presence of the NH_2 group and the degree of deacetylation [69].

Curcumin has antioxidant activity at low concentrations but at higher concentrations, it can ironically, act as a prooxidant compound, which is preferred in cancer therapy [19]. Curcumin's antioxidant activity may be attributed to its high polyphenol content, which acts as a donors for electrons or hydrogen and can stabilize the unpaired electrons and finish the Fenton reactions [70].

Cytotoxicity

A cytotoxicity experiment was performed to estimate the toxicity of oxidized MWCNTs as well as the therapeutic effect of curcumin after loading on either oxidized-MWCNTs or chitosan-functionalized MWCNTs against Fibroblast (normal cells) and Hep G2 (liver cancer cell line).

A conventional MTT assay was used to analyze the cytotoxicity of oxidized-MWCNT with and without chitosan functionalization, chitosan-MWCNTs with and

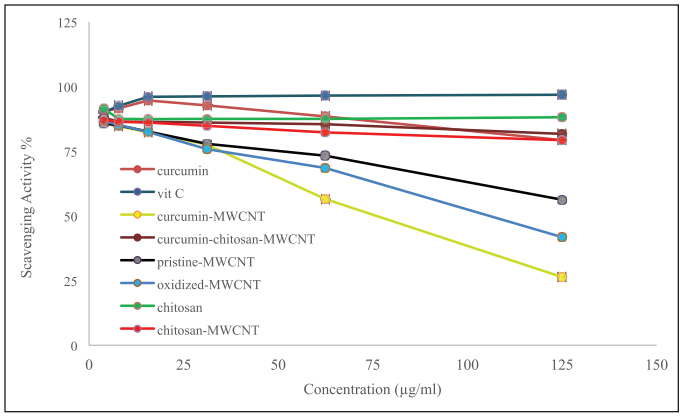

Figure 5. The DPPH radical scavenging activity of (A) oxidized-MWCNT chitosan, and chitosan-MWCNT compared to ascorbic acid (positive control), (B) curcumin, curcumin-MWCNT, and curcumin-chitosan-MWCNT compared to ascorbic acid. Bars represent the standard error of the mean.

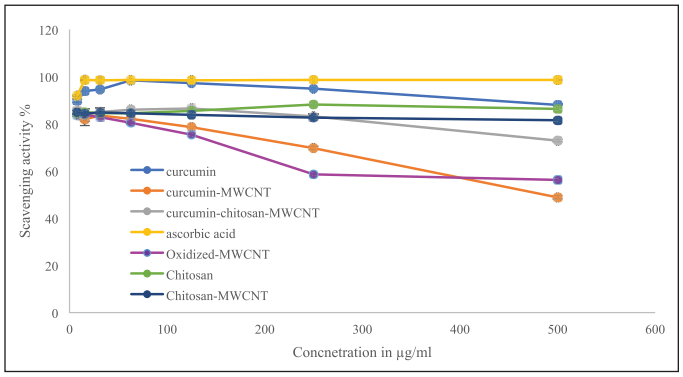

Figure 6. The ABTS radical scavenging activity of (A) oxidized-MWCNT, chitosan, and chitosan-MWCNT, compared with ascorbic acid (positive control), (B) curcumin, curcumin-MWCNT, and curcumin-chitosan-MWCNT compared to ascorbic acid. Bars represent the standard error of the mean.

without curcumin, curcumin-MWCNT, free chitosan, and free curcumin, against fibroblast and Hep G2 cells. These experiments were performed initially on fibroblast cells as six serial concentrations started from 400 µg/ml until 12.5 µg/ml as illustrated in Figure 7, then the same treatments were applied to the Hep G2 liver cancer cell lines.

Some viability assays, such as MTT, have been demonstrated to give false-positive results when employed with CNTs due to the attachment of formazan to the CNTs surface, which reduces its solubilization in the cell medium; therefore, before adding the MTT dye, the cell medium was removed and the cell wall was washed by PBS [71].

Figure 7 shows the viability of fibroblast, and Hep G2 cells after 72 hours of incubation with different concentrations from oxidized-MWCNT, chitosan, curcumin, chitosan-MWCNT, curcumin-chitosan-MWCNT, and curcumin-MWCNT. Approximately, 68.50% of fibroblast (Normal cells) were viable after treatment with 400 µg/ml of oxidized MWCNT compared with the Hep G2 cell line which showed low viability (25.8%) at high concentrations while decreasing concentrations of oxidized-MWCNT increased Hep G2 cell viability (Fig. 6A). The toxicity of oxidized MWCNT was reduced after functionalization with chitosan as presented in (Fig. 6D). Chitosan was noncovalently bound to MWCNT to improve biocompatibility [72].

Cancer cells had lower cell viability behavior after being treated with curcumin-chitosan-MWCNT compared with fibroblast, which might confirm the release behavior of curcumin. Both curcumin-MWCNT and curcumin-chitosan-MWCNTs demonstrated a dose-dependent fatal effect on fibroblast cells. Nevertheless, curcumin-chitosan-MWCNTs had more cytotoxicity than curcumin-MWCNT at the same dose. This is due to an increase in curcumin-chitosan-MWCNTs cellular uptake, which leads to an increase in curcumin accumulation within fibroblast cells [73].

In general, Hep G2 showed lower viability than fibroblasts (Fig. 7). For instance, after incubation with 200 µg/ml of curcumin-chitosan-MWCNTs, the viability of Hep G2 cells was 18.22%, while fibroblast cell viability was 45.6%. The enhanced cytotoxicity could be due to an increase in curcumin accumulation inside Hep G2 cells. Furthermore, the IC 50 of curcumin-chitosan-MWCNT was approximately two-fold lower than that of curcumin alone, and approximately nine-folds lower than that of curcumin-MWCNT (Table 4). This proves the increased anticancer activity of curcumin loaded onto chitosan-MWCNTs compared to that of free curcumin, suggesting that the combination between curcumin-chitosan-MWCNT increased the accumulation of curcumin in Hep G2 cancer cells and thus suppress their growth significantly.

For fibroblast cells, the highest cytotoxicity percentage was 60.12% which was achieved when treating fibroblast cells with 200 µg/ml oxidized-MWCNT, whereas treating them with chitosan gave the highest cytotoxicity percentage at 400 µg/ml which was 76.4%; however, at 200 µg/ml chitosan resulted in 61.49% cytotoxicity, which was approximately the same with that of oxidized-MWCNT at this concentration, while the combination between chitosan and MWCNT showed increased cytotoxicity % (77.10%) at the same concentration (200 µg/ml).

Between 400 and 50 µg/ml, curcumin exhibited higher than 80% cytotoxicity, while combining curcumin with MWCNT gave no cytotoxicity at 400 µg/ml, and between 12.5 and 200 µg/ml, it exhibited 10%–29% toxicity, which means that MWCNT is safe on fibroblast cells and decreases the toxicity of curcumin on cells after combination. Regarding curcumin-chitosan-MWCNT, this combination showed a dose-dependent manner Figure 7.

Regarding the Hep G2 liver cancer cell line, 74.21% was the highest cytotoxicity percentage achieved when treating cells with 400 µg/ml oxidized-MWCNT, and the highest chitosan cytotoxicity was 88.37% obtained at 400 µg/ml. However, 92.14%, 87.31%, 87.85%, and 75.2% were the highest obtained cytotoxicity for Hep G2 cells treated with 400 µg/ml curcumin, chitosan-MWCNT, curcumin-chitosan-MWCNT, and curcumin-MWCNT, respectively. They exhibited a fatal dose-dependent effect as the increased concentration gave the highest cytotoxicity on the liver cancer cell line (Hep G2).

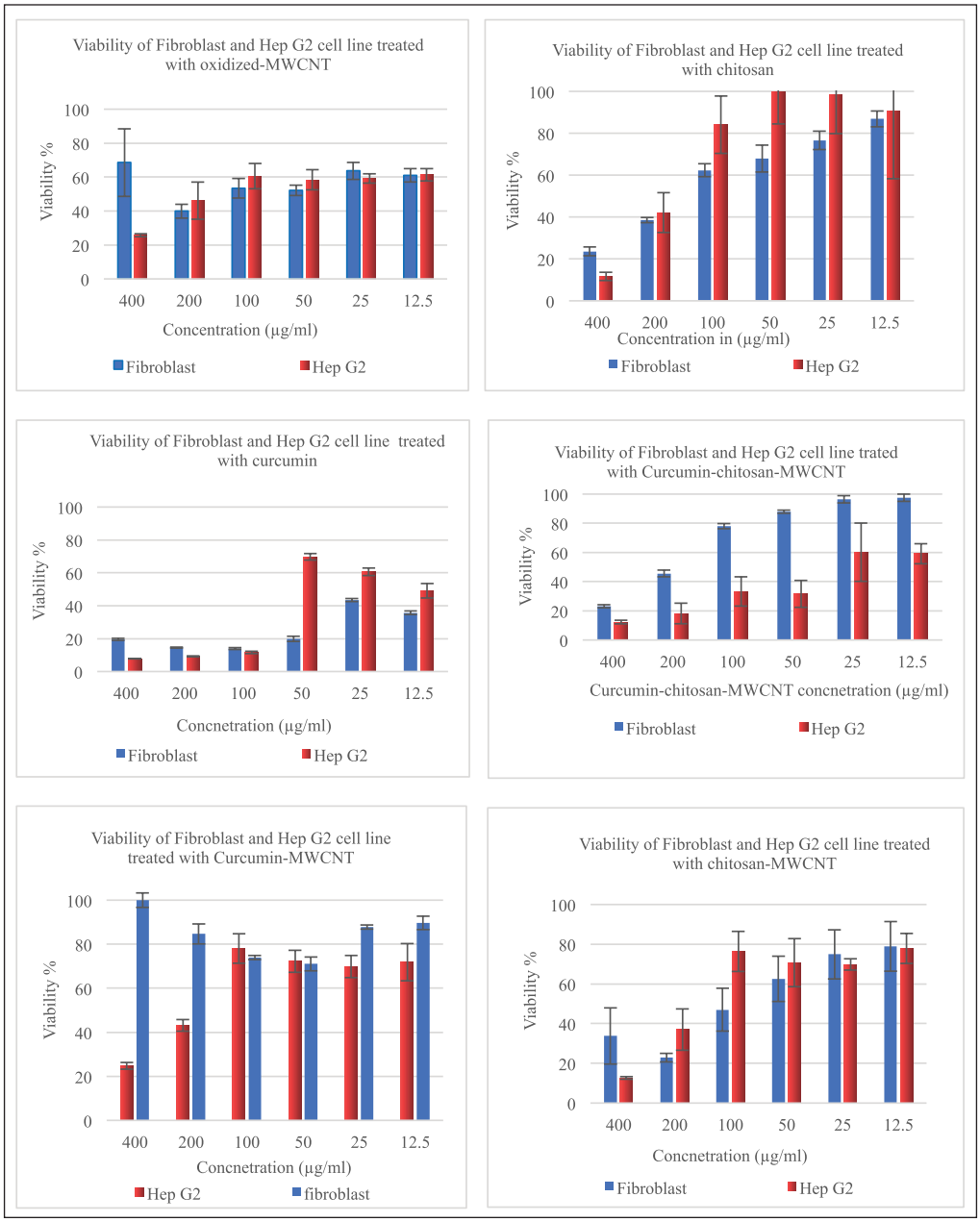

Figure 7. Viability of fibroblast, and Hep G2 after incubation for 72 hours with different concentrations of oxidized-MWCNT, chitosan, curcumin, chitosan-MWCNT, curcumin-chitosan-MWCNT, and curcumin-MWCNT.

Table 4. The IC 50 (µg/ml) values of oxidized-MWCNT, chitosan, curcumin, chitosan-MWCNT, curcumin-chitosan-MWCNT, and curcumin-MWCNT on fibroblast (normal cell line) and Hep G2 (liver cancer cell line).

Cell line	Fibroblast	Hep G2
Oxidized-MWCNT	1.112	469.4
Chitosan	103	285.1
Curcumin	5.468	91.18
Chitosan-MWCNT	41.01	336.7
Curcumin-Chitosan-MWCNT	227.6	43.62
Curcumin-MWCNT	Unstable	398.8

CONCLUSION

MWCNTs are considered an ideal drug delivery system; however, due to their insolubility in aqueous, solutions they were surface-functionalized before they were used in biomedical applications. In this study, MWCNTs biocompatibility was improved by chitosan-functionalization. After that chitosan-MWCNTs were coupled with curcumin, and their coupling was confirmed using FTIR, BET, TGA, and SEM, and their antioxidant activity was tested by DPPH and $ABTS^{+}$ methods, and showed that curcumin-chitosan-MWCNTs has more than 80% antioxidant activity for all used concentrations. The *in vitro* cytotoxicity of curcumin-chitosan-MWCNTs

and curcumin-MWCNT were examined against Hep-G2 and fibroblast, which express higher cytotoxicity than curcumin alone as the IC50 of curcumin was 91.18 µg/ml while that of curcumin-chitosan-MWCNT was 43.62 µg/ml, whereas 398.8 µg/ml was for curcumin-MWCNT against Hep G2 liver cancer cell line. This study demonstrated that chitosan-MWCNT can be used to improve curcumin antioxidant activity and enhance its delivery to the cancer microenvironment.

AUTHOR CONTRIBUTIONS

All authors made substantial contributions to conception and design, acquisition of data, or analysis and interpretation of data; took part in drafting the article or revising it critically for important intellectual content; agreed to submit to the current journal; gave final approval of the version to be published; and agree to be accountable for all aspects of the work. All the authors are eligible to be an author as per the International Committee of Medical Journal Editors (ICMJE) requirements/guidelines.

FINANCIAL SUPPORT

There is no funding to report.

CONFLICTS OF INTEREST

The authors report no financial or any other conflicts of interest in this work.

ETHICAL APPROVALS

This study does not involve experiments on animals or human subjects.

DATA AVAILABILITY

All data generated and analyzed are included in this research article.

PUBLISHER'S NOTE

This journal remains neutral with regard to jurisdictional claims in published institutional affiliation.

REFERENCES

1. Sobh RA, Nasr HES, Mohamed WS. Formulation and *in vitro* characterization of anticancer drugs encapsulated chitosan/multi-walled carbon nanotube nanocomposites. J Appl Pharm Sci. 2019;9(8):32–40.
2. AlKhatib HS, Taha MO, Aiedeh KM, Bustanji Y, Sweileh B. Synthesis and *in vitro* behavior of iron-crosslinked N-methyl and N-benzyl hydroxamated derivatives of alginic acid as controlled release carriers. Eur Polym J. 2006;42(10):2464–74.
3. Khdair A, Hamad I, Alkhatib H, Bustanji Y, Mohammad M, Tayem R, *et al.* Modified-chitosan nanoparticles: novel drug delivery systems improve oral bioavailability of doxorubicin. Eur J Pharm Sci. 2016;93:38–44.
4. Lafi Z, Alshaer W, Hatmal MM, Zihlif M, Alqudah DA, Nsairat H, *et al*. Aptamer-functionalized pH-sensitive liposomes for a selective delivery of echinomycin into cancer cells. RSC Adv. 2021;11(47):29164–77.
5. Matalqah SM, Aiedeh K, Mhaidat NM, Alzoubi KH, Bustanji Y, Hamad I. Chitosan nanoparticles as a novel drug delivery system: a review article. Curr Drug Targets. 2020;21(15):1613–24.
6. Alshaer W, Zraikat M, Amer A, Nsairat H, Lafi Z, Alqudah DA, *et al*. Encapsulation of echinomycin in cyclodextrin inclusion complexes into liposomes: *in vitro* anti-proliferative and anti-invasive activity in glioblastoma. RSC Adv. 2019;9(53):30976–88.
7. Gharaibeh L, Alshaer W, Wehaibi S, Al Buqain R, Alqudah DA, Al-Kadash A, *et al*. Fabrication of aptamer-guided siRNA loaded lipopolyplexes for gene silencing of notch 1 in MDA-mb-231 triple negative breast cancer cell line. J Drug Deliv Sci Technol. 2021;65:102733.
8. Nivethaa EAK, Dhanavel S, Rebekah A, Narayanan V, Stephen A. A comparative study of 5-fluorouracil release from chitosan/silver and chitosan/silver/MWCNT nanocomposites and their cytotoxicity towards MCF-7. Mater Sci Eng C. 2016;66:244–50.
9. Zawawi NA, Majid ZA, Rashid NAA. Adsorption and desorption of curcumin by poly(vinyl) alcohol-multiwalled carbon nanotubes (PVA-MWCNT). Colloid Polym Sci. 2017;295(10):1925–36.
10. Rosca ID, Watari F, Uo M, Akasaka T. Oxidation of multiwalled carbon nanotubes by nitric acid. Carbon. 2005;43(15):3124–31.
11. Avilés F, Cauich-Rodríguez JV, Moo-Tah L, May-Pat A, Vargas-Coronado R. Evaluation of mild acid oxidation treatments for MWCNT functionalization. Carbon. 2009;47(13):2970–5.
12. Dubey R, Dutta D, Sarkar A, Chattopadhyay P. Functionalized carbon nanotubes: synthesis, properties and applications in water purification, drug delivery, and material and biomedical sciences. Nanoscale Adv. 2021;3(20):5722–44.
13. Yang S, Shao D, Wang X, Hou G, Nagatsu M, Tan X, *et al*. Design of chitosan-grafted carbon nanotubes: evaluation of how the -OH functional group affects Cs+ adsorption. Mar Drugs. 2015;13(5):3116–31.
14. Noordadi M, Mehrnejad F, Sajedi RH, Jafari M, Ranjbar B. The potential impact of carboxylic-functionalized multi-walled carbon nanotubes on trypsin: a comprehensive spectroscopic and molecular dynamics simulation study. PLoS One. 2018;13(6):e0198519.
15. Wolski P, Nieszporek K, Panczyk T. Pegylated and folic acid functionalized carbon nanotubes as pH controlled carriers of doxorubicin. Molecular dynamics analysis of the stability and drug release mechanism. Phys Chem Chem Phys. 2017;19(13):9300–12.
16. Sangsanoh P, Supaphol P. Stability improvement of electrospun chitosan nanofibrous membranes in neutral or weak basic aqueous solutions. Biomacromolecules. 2006;7(10):2710–4.
17. Wang JJ, Zeng ZW, Xiao RZ, Xie T, Zhou GL, Zhan XR, *et al*. Recent advances of chitosan nanoparticles as drug carriers. Int J Nanomed. 2011;6:765–74.
18. Aiedeh KM, Taha MO, Al-Hiari Y, Bustanji Y, Alkhatib HS. Effect of ionic crosslinking on the drug release properties of chitosan diacetate matrices. J Pharm Sci. 2007;96(1):38–43.
19. Abadi AJ, Mirzaei S, Mahabady MK, Hashemi F, Zabolian A, Hashemi F, *et al*. Curcumin and its derivatives in cancer therapy: potentiating antitumor activity of cisplatin and reducing side effects. Phytother Res. 2022;36(1):189–213.
20. Bustanji Y, Taha MO, Almasri IM, Al-Ghussein MAS, Mohammad MK, Alkhatib HS. Inhibition of glycogen synthase kinase by curcumin: investigation by simulated molecular docking and subsequent *in vitro*/*in vivo* evaluation. J Enzyme Inhib Med Chem. 2009;24(3):771–8.
21. Mohammad M, Kasabri V, Zalloum H, Tayyem R, Aburish E, Al-Hiari Y, *et al*. Antilipolytic property of curcumin: molecular docking and kinetic assessment. Rev Roumaine Chim. 2015;60(10):983–9.
22. Asif HM, Zafar F, Ahmad K, Iqbal A, Shaheen G, Ansari KA, *et al*. Synthesis, characterization and evaluation of anti-arthritic and anti-inflammatory potential of curcumin loaded chitosan nanoparticles. Sci Rep. 2023;13(1):10274.
23. Law SK, Leung AWN, Xu CS. Curcumin and nanocurcumin in the treatment of photodynamic therapy for skincare. Lett Appl NanoBioSci. 2023;12(4):92–6.
24. Dytrych P, Kejík Z, Hajduch J, Kaplánek R, Veselá K, Kučnirová K, *et al*. Therapeutic potential and limitations of curcumin as antimetastatic agent. Biomed Pharmacother. 2023;163:114758.

25. Hao M, Chu Y, Lei J, Yao Z, Wang P, Chen Z, *et al*. Pharmacological mechanisms and clinical applications of curcumin: update. Aging Dis. 2023;14(3):716–49.
26. Jiang T, Liao W, Charcosset C. Recent advances in encapsulation of curcumin in nanoemulsions: a review of encapsulation technologies, bioaccessibility and applications. Food Res Int. 2020;132:109035.
27. Sanidad KZ, Sukamtoh E, Xiao H, McClements DJ, Zhang G. Curcumin: recent advances in the development of strategies to improve oral bioavailability. Annu Rev Food Sci Technol. 2019;10:597–617.
28. Bozeya A, Makableh YF, Abu-Zurayk R, Khalaf A, Bawab AA. Thermal and structural properties of high density polyethylene/carbon nanotube nanocomposites: a comparison study. Chemosensors. 2021;9(6):136.
29. Doğan M, Sabaz P, Bicil Z, Koçer Kizilduman B, Turhan Y. Activated carbon synthesis from tangerine peel and its use in hydrogen storage. J Energy Inst. 2020;93(6):2176–85.
30. Valot P, Baba M, Nedelec JM, Sintes-Zydowicz N. Effects of process parameters on the properties of biocompatible ibuprofen-loaded microcapsules. Int J Pharm. 2009;369(1–2):53–63.
31. Wu L, Man C, Wang H, Lu X, Ma Q, Cai Y, et al. PEGylated multi-walled carbon nanotubes for encapsulation and sustained release of oxaliplatin. Pharm Res. 2013;30(2):412–23.
32. Chaves N, Santiago A, Alías JC. Quantification of the antioxidant activity of plant extracts: analysis of sensitivity and hierarchization based on the method used. Antioxidants. 2020;9(1):76.
33. Harb AA, Bustanji YK, Abdalla SS. Hypocholesterolemic effect of β-caryophyllene in rats fed cholesterol and fat enriched diet. J Clin Biochem Nutr. 2018;62(3):230–7.
34. Mohammad MK, Almasri IM, Tawaha K, Issa A, Al-Nadaf A, Hudaib M, *et al*. Antioxidant, antihyperuricemic and xanthine oxidase inhibitory activities of *Hyoscyamus* reticulatus. Pharm Biol. 2010;48(12):1376–83.
35. Althaher AR, Oran SA, Bustanji YK. Chemical composition, *in vitro* evaluation of antioxidant properties and cytotoxic activity of the essential oil from *Calamintha incana* (Sm.) helder (Lamiaceae). Trop J Nat Prod Res. 2021;5(8):1333–9.
36. Wagay JA, Alanazi AM, Vyas D, Pala S, Rahman QI. Antioxidant and organic acid evaluation of Geaster saccatum mushroom by chemical and electrochemical assay at carbon nanotube paste electrode. J King Saud Univ Sci. 2021;33(2021):101336.
37. Arabiyat S, Kasabri V, Al-Hiari Y, Bustanji YK, Albashiti R, Almasri IM, *et al*. Antilipase and antiproliferative activities of novel fluoroquinolones and triazolofluoroquinolones. Chem Biol Drug Des. 2017;90(6):1282–94.
38. Belkacem N, Khettal B, Hudaib M, Bustanji Y, Abu-Irmaileh B, Amrine CSM. Antioxidant, antibacterial, and cytotoxic activities of *Cedrus atlantica* organic extracts and essential oil. Eur J Integr Med. 2021;42:101292.
39. Doğan M, Selek A, Turhan O, Kızılduman BK, Bicil Z. Different functional groups functionalized hexagonal boron nitride (h-BN) nanoparticles and multi-walled carbon nanotubes (MWCNT) for hydrogen storage. Fuel. 2021;303:121335.
40. Gohari MS, Rezaei SA, Rashidi A, Saremi M, Ebadzadeh T. The effect of mullite coating and microwave sintering on high temperature oxidation resistance of MWCNTs. Ceram Int. 2022;48(10):14281–7.
41. Waqas MK, Safdar S, Buabeid M, Ashames A, Akhtar M, Murtaza G. Alginate-coated chitosan nanoparticles for pH-dependent release of tamoxifen citrate. J Exp Nanosci. 2022;17(1):522–34.
42. Zhao X, Tian K, Zhou T, Jia X, Li J, Liu P. PEGylated multi-walled carbon nanotubes as versatile vector for tumor-specific intracellular triggered release with enhanced anti-cancer efficiency: optimization of length and PEGylation degree. Colloids Surf B Biointerfaces. 2018;168:43–9.
43. Ziegler KJ, Gu Z, Peng H, Flor EL, Hauge RH, Smalley RE. Controlled oxidative cutting of single-walled carbon nanotubes. J Am Chem Soc. 2005;127(5):1541–7.
44. Li H, Zhang N, Hao Y, Wang Y, Jia S, Zhang H, *et al*. Formulation of curcumin delivery with functionalized single-walled carbon nanotubes: characteristics and anticancer effects *in vitro*. Drug Deliv. 2014;21(5):379–87.
45. Abdolmaleki A, Mallakpour S, Rostami M. Surface modification of MWCNTs with glucose and their utilization for the production of environmentally friendly nanocomposites using biodegradable poly(amide-imide) based on N-trimellitylimido-S-valine matrix. Polym Adv Technol. 2015;26(9):1141–7.
46. Szymańska E, Winnicka K. Stability of chitosan—a challenge for pharmaceutical and biomedical applications. Mar Drugs. 2015;13(4):1819–46.
47. Hsieh CT, Teng H, Chen WY, Cheng YS. Synthesis, characterization, and electrochemical capacitance of amino-functionalized carbon nanotube/carbon paper electrodes. Carbon. 2010;48(15):4219–29.
48. Nandiyanto ABD, Oktiani R, Ragadhita R. How to read and interpret ftir spectroscope of organic material. Indones J Sci Technol. 2019;4(1):97–118.
49. Chang AKT, Frias RR, Alvarez LV, Bigol UG, Guzman JPMD. Comparative antibacterial activity of commercial chitosan and chitosan extracted from *Auricularia* sp. Biocatal Agric Biotechnol. 2019;17:189–95.
50. Hao X, Chen S, Yu H, Liu D, Sun W. Metal ion-coordinated carboxymethylated chitosan grafted carbon nanotubes with enhanced antibacterial properties. RSC Adv. 2015;6(1):39–43.
51. Zhou Y, Pervin F, Lewis L, Jeelani S. Fabrication and characterization of carbon/epoxy composites mixed with multi-walled carbon nanotubes. Mater Sci Eng A. 2008;475(1–2):157–65.
52. Su F, Lu C, Hu S. Adsorption of benzene, toluene, ethylbenzene and p-xylene by NaOCl-oxidized carbon nanotubes. Colloids Surf A Physicochem Eng Asp. 2010;353(1):83–91.
53. Koupaei Malek S, Gabris MA, Hadi Jume B, Baradaran R, Aziz M, Karim KJBA, *et al*. Adsorption and *in vitro* release study of curcumin form polyethyleneglycol functionalized multi walled carbon nanotube: kinetic and isotherm study. DARU J Pharm Sci. 2019;27(1):9–20.
54. Tofighy MA, Mohammadi T. Adsorption of divalent heavy metal ions from water using carbon nanotube sheets. J Hazard Mater. 2011;185(1):140–7.
55. Jun LY, Mubarak NM, Yon LS, Bing CH, Khalid M, Abdullah EC. Comparative study of acid functionization of carbon nanotube via ultrasonic and reflux mechanism. J Environ Chem Eng. 2018;6(5):5889–96.
56. Lau CH, Cervini R, Clarke SR, Markovic MG, Matisons JG, Hawkins SC, *et al*. The effect of functionalization on structure and electrical conductivity of multi-walled carbon nanotubes. J Nanopart Res. 2008;10(SUPPL. 1):77–88.
57. Datsyuk V, Kalyva M, Papagelis K, Parthenios J, Tasis D, Siokou A, *et al*. Chemical oxidation of multiwalled carbon nanotubes. Carbon. 2008;46(6):833–40.
58. Abuilaiwi FA, Laoui T, Al-Harthi M, Atieh MA. Modification and functionalization of multiwalled carbon nanotube (MWCNT) via fischer esterification. Arab J Sci Eng. 2010;35(1 C):37–48.
59. Arunkumar T, Karthikeyan R, Ram Subramani R, Viswanathan K, Anish M. Synthesis and characterisation of multi-walled carbon nanotubes (MWCNTs). Int J Ambient Energy. 2020;41(4):452–6.
60. Salehi Ardali N, Riahi S, Abbasi M, Mohammadpour N. Experimental investigation of carbon dioxide adsorption using functionalized MWCNTs with 1,6-diaminohexane. Fuel. 2023;338:127213.
61. Guo M, Wang J, Wang C, Strong PJ, Jiang P, Ok YS, *et al*. Carbon nanotube-grafted chitosan and its adsorption capacity for phenol in aqueous solution. Sci Total Environ. 2019;682:340–7.
62. Hsan N, Dutta PK, Kumar S, Das N, Koh J. Capture and chemical fixation of carbon dioxide by chitosan grafted multi-walled carbon nanotubes. J CO2 Util. 2020;41:101237.
63. Abdel Salam M, Gabal MA, Obaid AY. In preparation and characterization of magnetic multi-walled carbon nanotubes/ferrite

nanocomposite and its application for the removal of aniline from aqueous solution. Synth Met. 2012;161(23–24):2651–8.
64. Slika L, Patra D. A short review on chemical properties, stability and nano-technological advances for curcumin delivery. Expert Opin Drug Deliv. 2020;17(1):61–75.
65. Aghababaei M, Ghoreyshi AA, Esfandiari K. Optimizing the conditions of multi-walled carbon nanotubes surface activation and loading metal nanoparticles for enhanced hydrogen storage. Int J Hydrog Energy. 2020;45(43):23112–21.
66. Vardakas P, Kartsonakis IA, Kyriazis ID, Kainourgios P, Trompeta AFA, Charitidis CA, *et al*. Pristine, carboxylated, and hybrid multi-walled carbon nanotubes exert potent antioxidant activities in *in vitro*-cell free systems. Environ Res. 2023;220:115156.
67. Francisco-Marquez M, Galano A, Martínez A. On the free radical scavenging capability of carboxylated single-walled carbon nanotubes. J Phys Chem C. 2010;114(14):6363–70.
68. Tomida H, Fujii T, Furutani N, Michihara A, Yasufuku T, Akasaki K, *et al*. Antioxidant properties of some different molecular weight chitosans. Carbohydr Res. 2009;344(13):1690–6.
69. Xie W, Xu P, Liu Q. Antioxidant activity of water-soluble chitosan derivatives. Bioorg Med Chem Lett. 2001;11(13):1699–701.
70. Bishayee A, Bhatia D, Thoppil RJ, Darvesh AS, Nevo E, Lansky EP. Pomegranate-mediated chemoprevention of experimental hepatocarcinogenesis involves Nrf2-regulated antioxidant mechanisms. Carcinogenesis. 2011;32(6):888–96.
71. Kong M, Chen XG, Xing K, Park HJ. Antimicrobial properties of chitosan and mode of action: a state of the art review. Int J Food Microbiol. 2010;144(1):51–63.
72. Mo Y, Wang H, Liu J, Lan Y, Guo R, Zhang Y, *et al*. Controlled release and targeted delivery to cancer cells of doxorubicin from polysaccharide-functionalised single-walled carbon nanotubes. J Mater Chem B. 2015;3(9):1846–55.
73. Qi X, Rui Y, Fan Y, Chen H, Ma N, Wu Z. Galactosylated chitosan-grafted multiwall carbon nanotubes for pH-dependent sustained release and hepatic tumor-targeted delivery of doxorubicin *in vivo*. Colloids Surf B Biointerfaces. 2015;133:314–22.

How to cite this article:
Rabba'a M, Abu-Zurayk R, Abu-Irmaileh B, Mallouh SA, Bustanji Y. *In vitro* studies on curcumin-loaded multiwalled carbon nanotubes antioxidant activities and cytotoxicity against Hep G-2 liver cancer cell lines. J Appl Pharm Sci. 2024;14(06):218–230.